

# Proton and charge transfer in the intercalating antitumour drug pazelliptine



Marie P. Fontaine-Aupart,<sup>\*a</sup> H  l  ne Laguitton-Pasquier,<sup>b</sup> Robert Pansu,<sup>b</sup> Laurence Brian,<sup>a</sup> Eric Renault,<sup>a</sup> Mike C. Marden,<sup>c</sup> Christian Rivalle<sup>d</sup> and Emile Bisagni<sup>d</sup>

<sup>a</sup> Laboratoire de Photophysique Mol  culaire, U.P.R. 3351 CNRS, B  t 213, Universit   Paris Sud, 91405 Orsay, France

<sup>b</sup> Laboratoire de Photophysique et Photochimie Supramol  culaire et Macromol  culaire, E.N.S. Cachan, U.R.A. 1906 CNRS, 92 Cachan, France

<sup>c</sup> Laboratoire de Physiologie Physiopathologie du globule rouge, U. 299 INSERM, H  pital de Bic  tre, 94275 Le Kremlin Bic  tre, France

<sup>d</sup> Laboratoire de Synth  se Organique, U.R.A. 1387 CNRS, Institut Curie Section Recherche, B  t 110-112, 91405 Orsay, France

The photophysical properties of the synthetic drug pazelliptine (PZE) have been investigated in order to characterize the geometric and electronic structure of the molecule bound to DNA. Whatever the pH of the solution, a proton transfer reaction occurs in the excited state: this leads to the excited 9-N monoprotinated form of PZE. Deexcitation of this excited species is mainly non-radiative. A study of the fluorescence properties of sterically hindered derivatives allows us to propose the existence of a twisted internal charge transfer state to explain this non-radiative deexcitation. The formation of this state occurs on the picosecond timescale ( $\tau \sim 200$  ps) when PZE is fully protonated ring nitrogens (*i.e.* in acidic aqueous solutions).

The acido-basic properties of PZE and five related amino and amino-substituted derivatives have been previously studied by spectroscopic measurements. The absorption, fluorescence spectra and the fluorescence quantum yields as a function of pH (range 2–12) and buffer concentration (50 mmol dm<sup>-3</sup> to 1 mol dm<sup>-3</sup>) have been measured. Three pK<sub>a</sub> values have been determined, at 5.5, 6.5 and 9.2. This is good evidence for PZE having an appropriate pK<sub>a</sub> when bound to a hydrophobic and/or a hydrophilic structure.

## Introduction

Among molecules with a pK<sub>a</sub> close to the physiological pH, potential antitumour drugs can be considered as particularly interesting examples. Indeed, the basic form of such molecules can accumulate in acidic compartments of cells.<sup>1</sup> In addition, the electrostatic properties of the polycations, which can result from the substitution of a polycyclic intercalating system, could reinforce the affinity for DNA and provide better intercalating properties. An example of such antitumour drugs is ellipticine, with a pK<sub>a</sub> = 7.4,<sup>2</sup> whose numerous derivatives have been synthesized.<sup>3–4</sup> In this family, the biological properties of the (dialkylamino)alkylamino derivatives are significantly increased when compared to ellipticine or non-substituted aza-ellipticine. Among these molecules, the pazelliptine (PZE), a 9-aza-ellipticine derivative bearing a 3-(diethylamino)propylamino side chain, exhibits important antitumour activities.<sup>5</sup> Its intercalation into DNA has been revealed *in vitro* and a higher affinity for A–T base pairs was observed.<sup>6</sup> However, the factors which account for the greater antitumour activity of PZE are not known.

Detailed knowledge of the physical and chemical properties of PZE are thus necessary in order to understand the biological function of the molecule at the molecular level and the nature of the interactions with DNA under various environmental conditions. For this purpose, we carried out a physico-chemical study of the drug in aqueous solution at various pH and buffer concentration values from the standpoint of its absorption and fluorescence properties. The absorption and fluorescence spectra and the photophysical constants  $\phi_f$  and  $\tau_f$  are determined for the first time to the best of our knowledge.

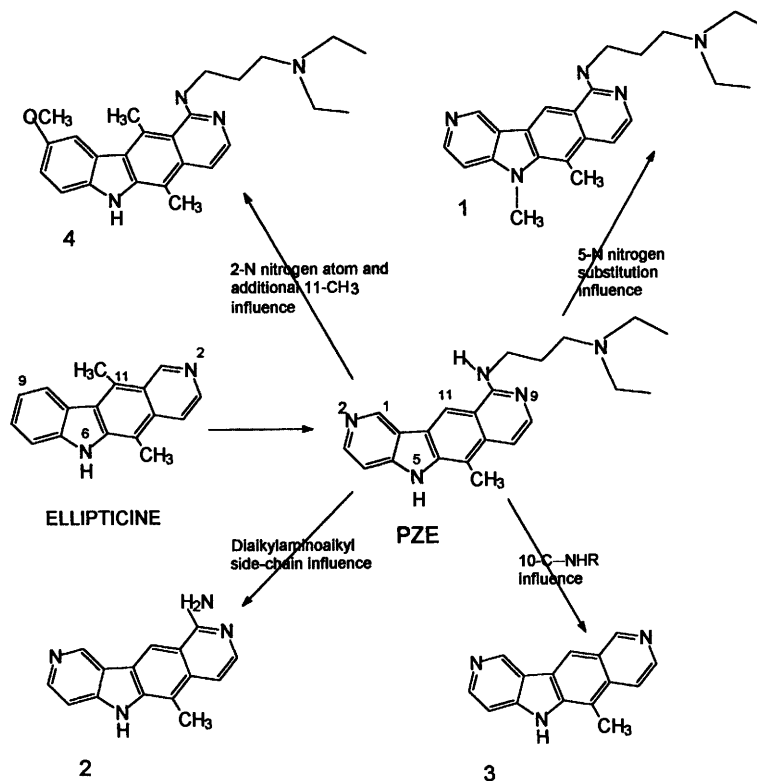
Using a comparative study of PZE and four related molecules (Scheme 1), the absorption bands have been assigned and the different pK<sub>a</sub> values attributed to each nitrogen atom, allowing the identification of the dominant proton repartition at different pH. At physiological pH, PZE is a monocation. However, we show that the charge is buried within the hydrocarbon chains due to an intramolecular hydrogen-bond.

Based on the observation of the fluorescence decays and quantum yields of PZE as a function of buffer concentration, it was first established that proton transfer occurred in the excited state, leading to a non-fluorescent species. In addition, an extra red emission band was observed in acidic solutions of PZE, revealing an ultrafast process in the excited state. Based on the comparison with PZE derivatives, this non-fluorescence species is suspected to be a twisted internal charge-transfer state, the nature of which is discussed.

## Experimental

### Chemicals

The chemical structures of the investigated molecules are represented in Scheme 1. The compounds were prepared as described in the literature.<sup>7</sup> For the pH influence study, the samples were dissolved in 0.04 mol dm<sup>-3</sup> phosphoric acid, boric acid and acetic acid (buffer A). The desired pH value from 2–12 was obtained by addition of an appropriate volume of NaOH at a concentration of 1 mol dm<sup>-3</sup>.<sup>8</sup> The dilution due to NaOH addition is small; nevertheless, the absorption spectra were corrected for this dilution. Phosphate buffer (KH<sub>2</sub>PO<sub>4</sub> pH 4, KH<sub>2</sub>PO<sub>4</sub>/K<sub>2</sub>HPO<sub>4</sub> pH 7) or carbonate buffer (pH 9) from



Scheme 1

50 mmol dm<sup>-3</sup> to 1 mol dm<sup>-3</sup> were used for the buffer concentration studies. Deoxygenated solutions were obtained by bubbling argon (from Alphagaz, 99.99%) through solutions. Salts are of analytical grade (Merck).

#### Absorption spectra

Ground state absorption spectra were recorded at 25 °C on a Perkin-Elmer spectrophotometer (Perkin-Elmer, Norwalk, CT) or a Cary 217 spectrophotometer (Varian) in quartz cuvettes of 1 × 1 cm cross section. The drug concentration was adjusted to obtain the absorbance value at 350 nm, varying from ca. 3 × 10<sup>-5</sup> to ca. 8 × 10<sup>-5</sup> mol dm<sup>-3</sup> according to the respective molecular mass of the molecules.

#### Fluorescence

Corrected steady-state emission and excitation spectra were obtained using an SLM spectrofluorometer (4 nm slits for both excitation and observation monochromators). Samples were temperature controlled at 25 °C. Fluorescence quantum yields ( $\phi_f$ ) were determined at  $\lambda_{exc} = 355$  nm, with 9,10-diphenylanthracene (DPA) in decalin solvent as reference ( $\lambda_{exc} = 355$  nm,  $\phi_f = 0.94$ ).<sup>9</sup> Typically, reference and samples were matched to have absorbances around 0.05 (optical pathlength 1 cm). Fluorescence quantum yields ( $\phi_f$ ) are calculated using the relationship in eqn. (1), where the x (subscript) refers to the unknown

$$\phi_{fx} = \phi_{fs} \frac{F_x A_x}{F_s A_s} \left( \frac{n_x}{n_s} \right)^2 \quad (1)$$

and *s* to the standard, *A* represents the absorbance at the excitation wavelength, *F* the integrated emission area across the band and *n<sub>x</sub>* and *n<sub>s</sub>* the refractive indexes of the respective solvents. The error on the fluorescence quantum yield was estimated to be 10%.

The time-resolved fluorescence measurements were performed using the third harmonic (355 nm) of a Q-switched Nd/YAG mode locked laser (BMI, 30 ps pulse width).<sup>10</sup> A monochromator and a streak camera interfaced with a microcomputer were used to measure the laser induced

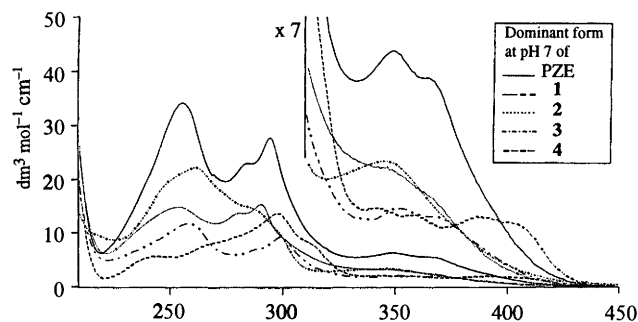


Fig. 1 Absorption spectra of PZE and compounds 1–4 in buffer A at pH 7.0; [PZE] = 3.32 × 10<sup>-5</sup>, [1] = 4.5 × 10<sup>-5</sup>, [2] = 3.27 × 10<sup>-5</sup>, [3] = 7.92 × 10<sup>-5</sup> and [4] = 3.26 × 10<sup>-5</sup> mol dm<sup>-3</sup>

emission signals at selected wavelengths as a function of time. The fluorescence decays present some dependence on the laser power. This latter was reduced by one order of magnitude to minimize this effect. Decay curves were fitted by least minimization with pulse deconvolution. The noise of the streak camera is a complex function of the acquisition time and gain conditions, and was not amenable to chi-squared evaluation.

## Results and discussion

#### Absorption spectra of PZE and its derivatives

The absorption spectra of PZE and the compounds 1–4 are illustrated in Fig. 1 in their dominant protonated form at pH 7.0. The PZE absorption spectra presents three main bands with peaks at 256, 295 and 350 nm with distinct vibrational structures.

Inspection of the absorption data for PZE and its derivatives reveals that the aza-ellipticine chromophore is insensitive to both the substitution with a methyl group at 5-N (compound 1) and the removal of the side chain (compound 2). The spectra of these two compounds closely resemble that of PZE with only an hypsochromic effect. For compound 3, which is the most simplified PZE derivative with the complete abstraction of the (dialkylamino)alkylamino side chain, the two main bands

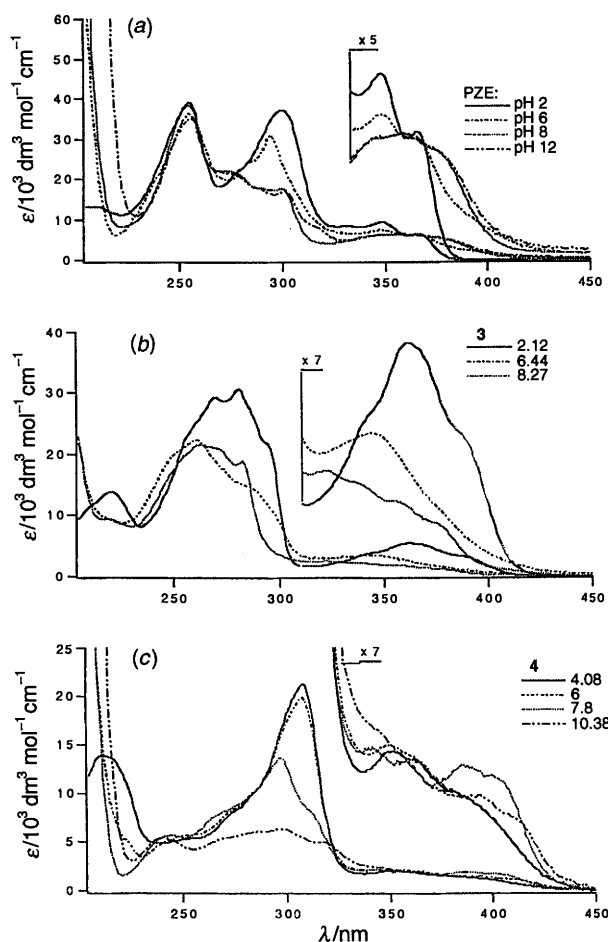


Fig. 2 Absorption spectra of (a) PZE, (b) compound 3 and (c) compound 4 in buffer A as a function of pH

centred at 256 and 295 nm have collapsed to one major band ( $\lambda_{\max} \sim 260$  nm) with a shoulder at 280 nm. The structural changes of compound 4, (replacement of 2-N nitrogen atom by a C-OCH<sub>3</sub> group and addition of a methyl group on 11-C) cause the disappearance of the highest absorption band at 254 nm and a red shift of the band centred at 350 nm (from 350 to 370 nm).

PZE has also pH dependent structural changes which can be followed from the absorption spectra [Fig. 2(a)]. In the pH range 2.0–7.0, the spectra are quite similar with only a decrease of the peak intensities and a gradual shift of the 305 nm maximum to 295 nm with increasing pH. Beyond pH 7.0, the disappearance of the 300 nm peak is observed. Moreover, the series of spectra at various pH from 2–12 gives different isosbestic points (see below) which clearly indicate that there are more than two structural forms of PZE.

The pH dependence of the absorbance properties of compounds 1–4 was also studied. The spectra of the compounds 1 and 2 closely resemble that obtained for PZE over the studied pH range. However, for compound 2, which has no  $pK_a$  above 6.5 (see below), its absorption spectrum does not evolve above pH 7. For compound 4, a pH increase from 5.0 to 9.5 considerably affects the band near 320 nm [Fig. 2(c)]. The peak intensity diminishes with increasing pH and an important blue shift of the maximum from 320 to 280 nm is observed. The absorption spectra of compound 3, in the pH range 2.0–5.0, are very different to those described at pH 7.0. The absorption increases with an important hypsochromic shift of all the peaks [10–20 nm, Fig. 2(b)]. Furthermore, a new band appears at 220 nm.

The comparative absorption spectra of PZE and its analogues as well as the effects of pH allow a phenomenological

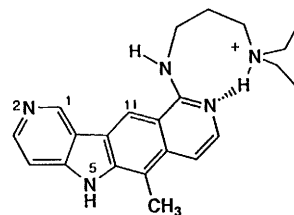


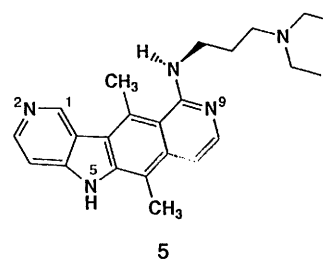
Fig. 3 Intramolecular hydrogen-bond in salified protonated PZE for  $7 < \text{pH} < 9.5$

attribution of the absorption bands to the different amino-groups of the molecules.

The first band centred at 350 nm, present for all the polyaza-aromatics, can be attributed to the polycyclic ring. This transition has some  $\pi$ - $\pi^*$  character, in agreement with the existence of a distinct vibronic progression and with the fluorescence results.

The second band around 300 nm is the most sensitive to pH. It is present for all the compounds but is blue shifted for compound 3. These observations allowed us to attribute to this band a contribution from the 9-N nitrogen atom for its blue part and from the amino-group for its red part.

The third band at 250 nm is insensitive to pH and non-existent for compound 4. Considering the structural modification of this molecule compared to PZE and compounds 1, 2 and 3, this absorption transition can be attributed either to the 2-N nitrogen atom or to the methyl group on 11-C. To resolve this question, the absorption of a new PZE derivative with a methyl group on 11-C (compound 5) was studied. The spectral



properties of compound 5 are similar to those of PZE, attesting that the absorption band centred at 250 nm is associated with the 2-N nitrogen atom.

The most surprising result is the sensitivity of the absorption spectra to the protonation state of the amino group of the side chain ( $pK_a$ , ca. 9.2, see below). This reveals that the lateral chain plays an important role in the molecular orbitals. The chain is too long to influence the aromatic ring by an inductive effect. Two types of interactions remain possible: a non-specific complex between the side chain and the polyaromatic cycle or a hydrogen-bond between the protonated form of the amino group and the deprotonated 9-N nitrogen atom of the chromophore as represented in Fig. 3. This second hypothesis is supported by our spectroscopic measurements. Indeed, the absorption spectra are modified in the pH domain where a hydrogen-bond might be expected (between pH 6.5–9.5) whereas a non-specific interaction would be seen at all pH values.

#### Determination and attribution of the $pK_a$ of PZE and its derivatives

The recording of the absorption spectra of PZE between pH 2–12 every 0.5 unit of pH reveals the presence of several isosbestic points in three pH domains: 2–6.5, 5.5–9 and 7.5–12, which clearly indicates that there are three equilibria between four structural forms of PZE. According to this observation, three  $pK_a$  values are expected.

At a fixed wavelength, the value of the  $pK_a$  is related to the

**Table 1** Ground state  $pK_a$  values and attribution for PZE and compounds 1–4

Compound	$pK_a$ 1 2-N	$pK_a$ 2		$pK_a$ 3 NR <sub>3</sub>
		10-C(NH <sub>2</sub> )-9-N	9-N	
PZE	5.5 ± 0.2 (5.8)	6.5 ± 0.2 (7.7)		9.2 ± 0.4 (9.8)
1	5.4 ± 0.3	6.4 ± 0.2		9.5 ± 0.5
2	5.4 ± 0.2	6.8 ± 0.4		
3	5.3 ± 0.2		7.5 ± 0.3	
4	5.3 ± 0.2	6.6 ± 0.4		9.7 ± 0.2
Ellipticine			7.4 <sup>b</sup>	

<sup>a</sup> Values calculated from absorbance data (values in parentheses calculated from fluorescence data). <sup>b</sup> For 2-N nitrogen (ref. 2).

pH and the absorbance by eqn. (2), where  $A_a$  and  $A_b$  represent the absorbance of the molecule in its acidic and basic forms,

$$pK_a = \text{pH} - \log \frac{A - A_a}{A_b - A} \quad (2)$$

respectively, and  $A$  the absorbance of the molecule at an intermediate pH. The different  $pK_a$  values obtained for PZE and the compounds 1–4 are listed in Table 1.

Fluorescence spectra of PZE as a function of pH reveal the existence of isoemissive points, thereby reflecting again equilibria between different forms of the molecules in the ground state. For comparison with the absorption data, the different  $pK_a$  of PZE are also determined from the fluorescence measurements and reported in the Table 1. We observe a good correlation between  $pK_a$  determination from absorption or emission spectra except for the value around 7.0. This discrepancy could be due to the buffer concentration values in the pH range 6.0–8.0 not being low enough to prevent proton transfer in the lowest excited state as described below.

The comparison of the stationary spectroscopic absorption properties of PZE and compounds 1–4 as a function of pH allows an attribution of the different  $pK_a$  of PZE and of its analogues (Table 1). The  $pK_a$  values are clustered in three pH regions around 5, 7 and 9. This shows that the  $pK_a$  properties of the aromatic nitrogens are independent and allows a step-by-step attribution of the  $pK_a$  values.

Previous works reported only one  $pK_a$  for ellipticine at 7.4.<sup>2</sup> Comparison of the ellipticine  $pK_a$  with those of compound 3, the most similar molecule, suggests the attribution of the  $pK_a = 7.5$  to the nitrogen 9-N [2-N in ellipticine (Scheme 1)]. Then the  $pK_a = 5.5$  of compound 3 can be attributed to the nitrogen 2-N. Indeed, deprotonation of the pyrrolo function is not possible at pH > 2.<sup>11</sup> Comparison of the  $pK_a$  values obtained for PZE and compounds 1–4 confirms the attribution of the  $pK_a$  at around 5 to the 2-N nitrogen and the one around 7 to the 9-N or 10-C(NH<sub>2</sub>)-9N group. Indeed, the proximity of the two nitrogen atoms allows one to consider only one acido-basic functional group with one  $pK_a$ , as in amidins. The rapid proton exchange between the two atoms is consistent with the lower value of the  $pK_a$  obtained for compounds having a 10-C(NH<sub>2</sub>)-9N group (PZE, compounds 1, 2 and 4) compared to compound 3 or ellipticine. For compound 4, a  $pK_a$  around 5 was suspected in view of the absorbance variations observed in the near UV domain (*ca.* 200 nm). This data is unexpected since in this compound the 2-N nitrogen atom is not present (Scheme 1). The result is at this time not interpreted but could be due to imprecision in the measurements in this spectral range. Referring to the literature,<sup>11</sup> the  $pK_a = 9.2$  could be attributed to the 5-N nitrogen of the pyrrole ring. However, this  $pK_a$  has also been determined for compound 2, for which the hydrogen is substituted by a methyl group, and not observed for compounds 2 and 3 with a hydrogen atom on 5-N. The  $pK_a = 9.2$ , is only observed for compounds having the (dialkyl-

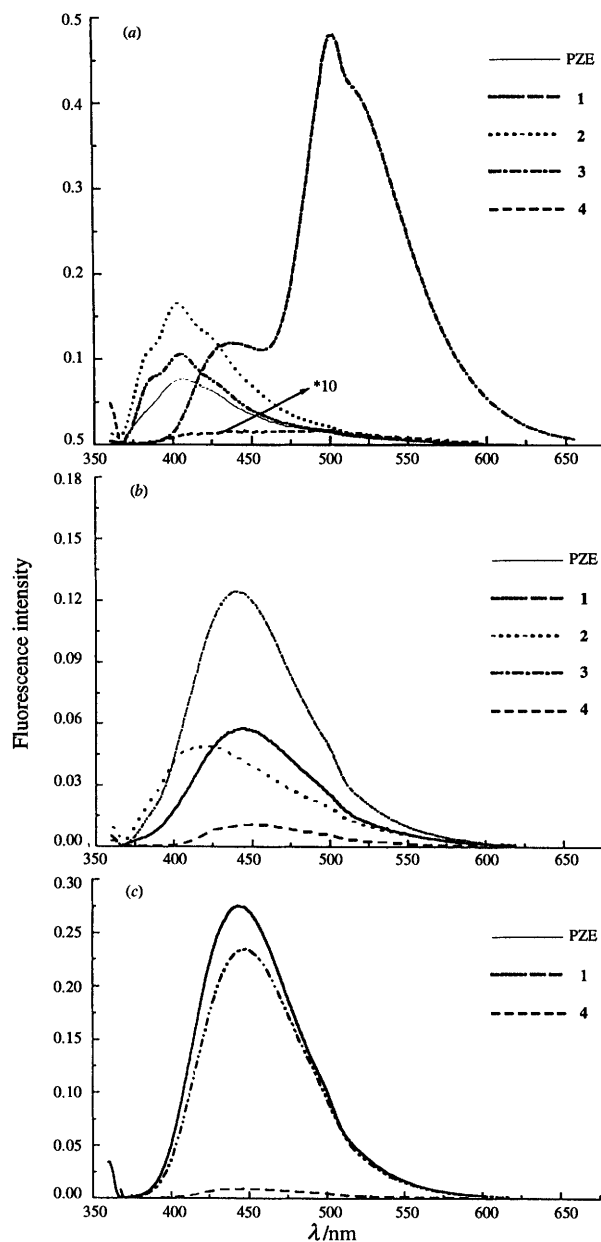


**Fig. 4** Emission spectra of PZE and compounds 1–4 in 50 mmol dm<sup>-3</sup> buffer as a function of pH ( $\lambda_{exc} = 355$  nm, absorption maximum of the first band for each compound); (a) pH 4.3, (b) pH 7.0 and (c) pH 9.9

amino)alkylamino side chain (PZE, compounds 1 and 4) and can be attributed to this function.

This  $pK_a$  determination revealed that PZE and its derivatives cannot be considered as an association of 5-azaindole ( $pK_a$  8.2)<sup>12–14</sup> and an isoquinoline ( $pK_a$  5.4).<sup>11</sup> The tetracyclic system forms a new entity with its own characteristic properties.

#### Fluorescence properties of PZE and its analogues

The stationary fluorescence spectra of PZE and its related derivatives as a function of pH are illustrated in Fig. 4. The emission spectrum of PZE in phosphate buffer (50 mmol dm<sup>-3</sup>, pH 7.0) shows a broad band centred at 440 nm. A gradual decrease of intensity for this emission maxima is observed with decreasing pH in the range 7–2 together with the appearance of another band at 400 nm [Fig. 4(a), (b)]. From pH 7 to 12, the emission maximum remains centred at 440 nm [Fig. 4(c)], but the fluorescence intensity increases as confirmed by the fluorescence quantum yield determination (Table 2).

The fluorescence emission properties of PZE were also obtained at different buffer concentrations, from 50 mmol dm<sup>-3</sup> to 1 mol dm<sup>-3</sup>. The buffer concentration influence on the

**Table 2** Emission maxima ( $\lambda_{\text{max}}$ ) and quantum yield ( $\phi_f$ ) for PZE, compounds 1–4 and ellipticine in buffer solutions at different pH

Compound	pH	Emission $\lambda_{\text{max}}$ /nm	Quantum yield $\phi_f$ ( $\pm 10\%$ )
Ellipticine <sup>a</sup>	4.3	525 (pH 6)	
PZE		405	0.084
1		400	0.15
2		400	0.24
3		500	0.73
4		No measurement	
Ellipticine	7.0	525	
PZE		445	0.15
1		440	0.21
2		420	0.14
3		445	0.2
4		450	0.02
Ellipticine	9.9	445	
PZE		445	0.544
1		450	0.46
3		440	
4		No measurement	

<sup>a</sup> Ref. 2.**Table 3** Maximum emission wavelengths ( $\lambda_{\text{max}}$ ) and quantum yields ( $\phi_f$ ) (relative to that determined in 50 mmol dm<sup>-3</sup> buffer solution) as a function of buffer

Buffer concentration/ mol dm <sup>-3</sup>	$\lambda_{\text{emi}}$ /nm	$\phi_f$
0.05	440	1.00
0.25	445	0.45
0.5	450	0.22
1	460	0.04

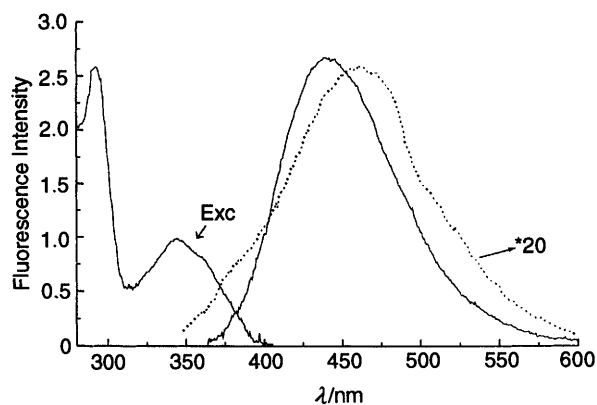
emission spectra is only observed at pH 7.0, where the maximum shifts from 440 to 470 nm when the buffer concentration increased from 50 mmol dm<sup>-3</sup> to 1 mol dm<sup>-3</sup> (Fig. 5). However, a decrease of the fluorescence quantum yield is observed with increasing buffer concentration whatever the pH (Table 3).

The fluorescence emission spectra of compounds 1–4 as a function of pH are also displayed in Fig. 4, and the maximum emission wavelengths and the fluorescence quantum yields are summarized in Table 2. The structural modifications of compounds 1 and 2 compared to PZE do not modify the fluorescence properties of these molecules in the range pH 2–12. This result substantiates the observation obtained from absorption spectroscopy. The same applies for compound 3 for pH higher than 7.0, whereas acidic conditions produce a decrease in the 440 nm peak and the appearance of a 500 nm peak correlated with an important increase of the quantum yield (Table 2). Compound 4 exhibits a weak fluorescence at pH 7.0. A quasi-total quenching is observed in acidic and basic conditions.

#### Fluorescence decay

The time resolved fluorescence spectra and decays for PZE and compounds 1–4 in different conditions of pH and buffer molarity were measured with excitation at 355 nm.

The fluorescence decays depend on the protonation state of PZE and, in the pH range 5.5–9.5, can be fitted by two or more exponentials (Table 4). These fluorescence decays are measured at concentrations where aggregation is absent, as shown by the agreement with the Beer–Lambert law. This complexity of the fluorescence decays can be explained by the presence of ground state tautomers as observed for 7-azaindole<sup>15</sup> or  $\beta$ -carboline.<sup>16</sup> The simultaneous excitation of these tautomers gives rise to multiexponential decays. Indeed in basic conditions (PZE

**Fig. 5** Emission spectra of PZE in phosphate buffer pH 7.0: (Exc.) excitation spectrum (emission at 440 nm); emission spectra (excitation at 355 nm) in 50 mmol dm<sup>-3</sup> buffer (solid line) and in 1 mmol dm<sup>-3</sup> buffer (dashed line). *Insert*: maximum emission wavelengths ( $\lambda_{\text{max}}$ ) and quantum yields ( $\phi_f$ ) (relative to that determined in 50 mmol dm<sup>-3</sup> buffer solution) as a function of buffer concentration.

totally deprotonated), where only one tautomer exists, no evolution of the emission spectrum is observed with time [Fig. 6(b), (d)]. The fluorescence decay could be fitted by the same single exponential at all wavelengths with a decay time depending on the buffer concentration as it is reported in Table 4.

In acidic medium, where again only one tautomer exists (PZE totally protonated), the fluorescence properties are more complex. The existence of an isoemissive point reveals the formation of a new species in the excited state with a red shift in its fluorescence compared to the initial molecule [Fig. 6(c)]. However, the fluorescence at 470 nm is always very low compared to that at 400 nm [Fig. 6(a)]. This result is consistent with the observation of the same fluorescent maximum in static and dynamic measurements. For  $\lambda < 450$  nm only a fluorescence decay is observed. When  $\lambda > 450$  nm, the fluorescence emission must be fitted to the form  $F(t) = -A \exp(-t/\tau_0) + B \exp(-t/\tau)$ , where  $\tau_0$  and  $\tau$  represent, respectively, the short- and long-lived components reported in Table 5. This rise cannot be attributed to the presence of different ground state species but is characteristic of an excited state reaction.

Compounds 1 and 2 in 50 mmol dm<sup>-3</sup> buffer yield fluorescence decays similar to those of PZE under the same experimental conditions (Table 5). The two fluorescence decay times measured for compound 3 are both longer than for the other molecules. For compound 4, a very weak time-resolved fluorescence decay can be detected at any pH but no rise in the emission is observed in acid medium.

The fluorescence properties of PZE in aqueous solutions are more complex than in non-polar solvents or alcohol.<sup>17</sup> Indeed, we have shown that over the pH range 2–12, the fluorescence quantum yields do not exceed 0.5 ( $\phi_f \sim 0.9$  in dioxane or ethanol), revealing other deactivation processes in competition with fluorescence. We have previously shown that this result cannot be explained by an increase in the intersystem crossing process which occurred with the same low yield in all the solvents.<sup>17</sup> Furthermore, the excited singlet state decay is multiexponential in aqueous solutions and monoexponential in dioxane or ethanol (Table 4) with substantially faster decay times. These results suggest a dynamic relaxation of PZE in aqueous solutions.

For all the molecules (PZE, compounds 1–4, ellipticine),<sup>18</sup> the fluorescence spectra drastically change upon protonation of the 9-N nitrogen atom. In acidic conditions, compound 3 and ellipticine have distinct spectroscopic properties compared to the others. For these two molecules,  $\phi_f$  and  $\tau_f$  increase significantly associated with an important red shift of the

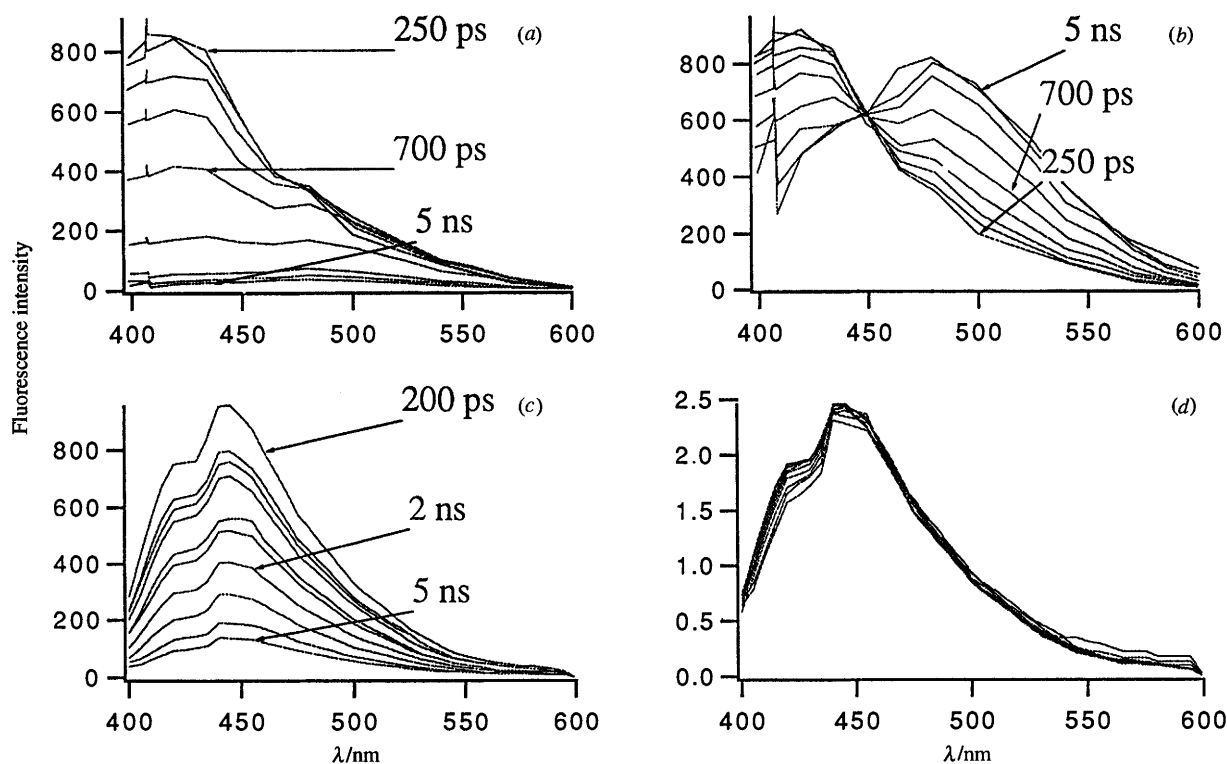


**Fig. 6** Time resolved fluorescence spectra of PZE in 50 mmol dm<sup>-3</sup> buffer solutions at (a) pH 4.3 and (b) pH 9.9. In order to facilitate observation of the spectral evolution from  $t = 200$  ps to  $t = 6$  ns, the spectra are normalized to the same area; (c) pH 4.3 and (d) pH 9.9.

**Table 4** Fluorescent kinetic data for PZE as a function of pH, buffer concentration and solvent nature

Buffer concentration/ mol dm <sup>-3</sup>	Emission decay time/ns	
	pH 4.3	pH 9.9
1	$\tau_0 = 0.2$ $\tau = 0.9$	$\tau = 2.7$
0.5	$\tau_0 = 0.2$ $\tau = 1.1$	$\tau = 4$
0.25	$\tau_0 = 0.2$ $\tau = 1.1$	$\tau = 5$
0.05	$\tau_0 = 0.2$ $\tau = 1.4$	$\tau = 6$
Dioxane	$\tau = 4.2$	
Ethanol	$\tau = 3.8$	

**Table 5** Fluorescence decay times of PZE and its analogues in acidic medium

Compound	Emission decay times at pH 4.3	
	$\tau_0$ /ps	$\tau$ /ns
PZE	200	1.4
<b>1</b>	200	1.3
<b>2</b>	50	3.3

maximum emission ( $\lambda_{\text{max}} = 500$  nm). This abnormally high Stokes shift suggests a modification of the molecule in the excited state. Indeed, the dynamic measurements for compound **3** reveal the formation of a new species with a lifetime  $\tau \sim 1.2$  ns, but no further information can be given at this time.

For PZE in acidic and basic medium, there is an obvious similarity with the behaviour of the excited species upon increasing buffer concentration. The emission spectra are practically unchanged but the fluorescence intensity and lifetimes decrease from 50 mmol dm<sup>-3</sup> to 1 mmol dm<sup>-3</sup> buffer (Tables 3 and 4). The fluorescence quenching follows the Stern-

Volmer equation [eqn. (3)], where  $\tau$  is the fluorescence decay

$$1/\tau = 1/\tau_f + k_t c_B \quad (3)$$

time in the presence of the quencher whose concentration is  $c_B$ ,  $\tau_f$  the fluorescence decay time for  $c_B = 0$  and  $k_t$  is the quenching constant (Fig. 7). The values of  $k_t$  are  $0.45 \times 10^9$  and  $0.227 \times 10^9$  dm<sup>3</sup> mol<sup>-1</sup> s<sup>-1</sup> at pH 4.3 and 9.9, respectively, that leads to  $\tau_f = 1.45$  ns at pH 4.3 and 6.7 ns at pH 9.9. These data are consistent with the occurrence of a proton transfer with the buffer and the formation of a non-fluorescent species. This is also in agreement with the lower quantum yield in water compared to ethanol and dioxane, where this proton transfer does not occur. These results are the basis of the global mechanism (Fig. 8) that is put forward for the excited state processes.

#### Proton transfer

At pH 9.9 and low buffer concentration, the fluorescence decay of the fully deprotonated PZE molecule is dominated by the emission of species V (Fig. 8) (lifetime 6.7 ns, maximum of emission 440 nm). At higher buffer concentration, the basic form V is protonated, probably on the 9-N nitrogen atom, to give the weakly fluorescent species IV (emission at 470 nm). This is consistent with the drop of the quantum yield and the appearance of a red shoulder at 470 nm on the fluorescence stationary spectrum. The emission of species IV at 470 nm can be seen by the direct excitation of PZE at pH 7 in 1 mol dm<sup>-3</sup> phosphate buffer (Fig. 5). Indeed, at this pH both the protonated and deprotonated forms of the 10-C(NH<sub>2</sub>)-9N group are present in solution and all the excited molecules are first converted into the species IV. At low buffer concentration, the emission of IV is masked by the stronger emission of the basic state V, explaining the emission maximum centred at 440 nm of the stationary spectrum. This species IV is ultimately converted into the species III identified from the studies in acidic medium as described below.

In acidic conditions, where no tautomeric PZE forms are expected in the ground state, the salient feature is the rise of a

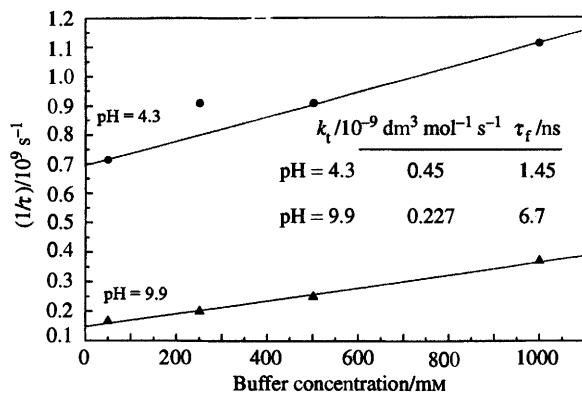


Fig. 7 Stern-Volmer representation of the PZE fluorescence as a function of buffer concentration at pH 4.3 and 9.9 ( $[PZE] = 2 \times 10^{-5} \text{ mol dm}^{-3}$ ).  $k_t$  is the quenching constant and  $\tau_f$  the fluorescence lifetime in absence of buffer.

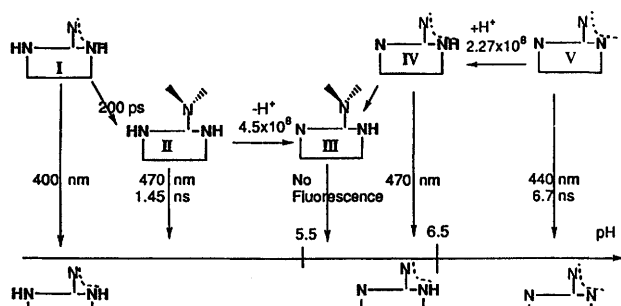


Fig. 8 Schematic representation of the excited state deactivation of PZE as a function of pH

red emission at *ca.* 470 nm (Fig. 6). This reaction, only detected for the totally protonated molecule, reveals the existence of an adiabatic reaction in the singlet excited state. The rise time is too short (200 ps) to measure the influence of buffer concentration. This picosecond process could correspond to the formation of an excited tautomer consecutive to a rapid proton transfer to a water molecule. Indeed, it has been reported<sup>19</sup> that excited polycations can behave as much stronger photoacids than the corresponding neutral molecules. The formation of a tautomer with the 5-N nitrogen atom could be considered. The presence of two protons on the 2-N and 9-N nitrogen atoms should lead to a more acid excited  $pK_a$  of the 5-N atom and to an ultrafast proton ejection to water. This loss of a proton coupled to intramolecular electron transfer could be 'the driving force' for the formation of an excited tautomer with 5-N. However, the appearance of the emissive red species at pH 4.3 is also observed for the compound **1** (Table 5) where 5-N is methylated. Thus the formation of an excited tautomer involving the deprotonation of 5-N is excluded. Considering an identical proton transfer scheme, a tautomer interconversion could also occur between the 2-N and 9-N nitrogen atoms consecutively to give the loss of a proton on 2-N. Nevertheless, it seems unreasonable that a fast initial proton transfer to water could favour the less stable excited tautomer. According to these arguments, the fast initial step whose rate seems independent of buffer concentration would be attributed to an intramolecular process. The fluorescence lifetime of the excited species thus formed depends on the buffer concentration (Table 4) revealing that the fast initial step is followed by a buffer-induced deprotonation on 2-N. According to Fig. 8, the acid form **I** gives the species **II** described later, which ultimately deprotonated to give the non-fluorescent species **III**.

#### Twisted internal charge transfer formation

One of the most surprising observations is the very weak fluorescence, at all pH values, of compounds **4** and **5** which

both have an additional methyl substituent at their 11-position compared to PZE. However, compound **5** and PZE show identical absorption properties. These results cannot be explained except by steric hindrance to the coplanarity of the amino-side chain (or the 10-amino group) and the polycyclic ring of the molecule, due to the adjunction of the 11-C methyl group, that favours a strongly twisted structure along the 10-C(NH<sub>2</sub>) bond in the ground state. This steric effect destabilizes the normal planar  $\pi\pi^*$  excited state leading to a non-radiative twisted state. This behaviour has also been observed on dimethylaminobenzonitrile (DMABN) derivatives.<sup>20,21</sup>

These experimental results reveal that the 10-C(NH<sub>2</sub>) group is susceptible to creation of a twisted internal charge transfer (TICT) state with the aromatic polycycle as observed for other aza-aromatic rings.<sup>21</sup> The adiabatic reaction, observed for PZE and compounds **1** and **2** in acidic medium, would correspond to the formation of this expected TICT state. The fluorescence properties of compound **3** and ellipticine in acidic conditions are also consistent with this TICT hypothesis. Indeed, the necessary coplanarity of these two molecules prevents any twisted excited-state transition resulting in their greater fluorescence yields. According to Fig. 8, the excited species **I** gives rise to the twisted excited species **II**, which fluoresces weakly with a maximum emission around 470 nm. Comparison of PZE with compounds **1** and **2** reveals that the side chain slows down the TICT formation rate (Table 4), probably due to the greater steric hindrance. The formation of the TICT state is favoured by the protonation of the 9-N nitrogen that increases the electron affinity of the polycyclic ring. This is supported by the results obtained in dioxane and ethanol or in basic conditions. When 9-N is deprotonated, the electron affinity of the aromatic ring might be not high enough to drive an electron from 10-C(NH<sub>2</sub>) to the ring. The molecules exhibit a fluorescence and no TICT formation is observed. After protonation of the 10-C(NH<sub>2</sub>)-9-N system by the buffer, the excited molecule twists to the non-fluorescent conformation **III**.

#### Biological relevance

We have found that the presence of a (dialkylamino)alkylamino side chain on the PZE molecule modifies the physico-chemical properties of the drug compared to that of the original model molecule ellipticine. At physiological pH (pH 7.4), PZE is not neutral, unlike ellipticine ( $pK_a = 7.3$ ). This provides the possibility of easily obtaining stable water-soluble salts, and therefore good solubility and bioavailability of the molecule. However, the spectroscopic study reveals the existence of an intramolecular hydrogen-bond between the charged lateral dialkylamino side chain and the neutral poly aza-aromatic core. In this conformation, the charge is spread over the entire molecular core, which is probably a more favourable conformation for transmembrane diffusion. On the other hand, in the tumour cell which corresponds to a more acidic environment, PZE is able to release its protected charge. These physico-chemical properties could explain why PZE diffuses toward DNA *in vivo* more easily than ellipticine.<sup>22</sup> Furthermore, in the neighbourhood of a polyanion such as DNA, PZE is able to be totally protonated. This provides the possibility of combining both stacking forces, involved in the intercalation complexes of ellipticine, with an electrostatic stabilization *via* the dibasic side chain and phosphate group interactions.

#### Conclusions

The comparative study of PZE and five related derivatives allows the characterization of the physico-chemical properties of the drug. The fluorescence quenching due to steric hindrance around the 10-C(NH<sub>2</sub>) group suggests the existence of a non-radiative TICT state in the 9-aza-ellipticine molecules. A process is proposed to describe the proton transfer that occurs in the excited molecule in acidic and basic medium.

Different protonated forms of PZE have been revealed by absorption spectroscopy. The three  $pK_a$  values of 5.5, 6.5 and 9.2 have been attributed respectively to the 2-N and 9-N nitrogen atoms, and to the alkylamino side chain. From the influence of the lateral chain on the absorption properties of PZE, the existence of an intramolecular hydrogen-bond is proposed which could have some correlation with the antitumour activity of the drug.

### References

- 1 G. Dodin, J. Pantigny, J. Aubart and M. A. Schwaller, *Anti-Cancer Drug Des.*, 1990, **5**, 129.
- 2 G. Dodin, M. A. Schwaller, J. Aubart and C. Paoletti, *Eur. J. Biochem.*, 1988, **176**, 371.
- 3 C. H. Nguyen, E. Bisagni, F. Lavelle, M. C. Bissery and C. Huel, *Anti-Cancer Drug Des.*, 1992, **7**, 219.
- 4 G. Behravan, M. Leijon, V. Sehlstedt, B. Norden, H. Vallberg, J. Bergman and A. Gräslund, *Biopolymers*, 1994, **34**, 599.
- 5 E. Moustacchi, V. Favaudon and E. Bisagni, *Cancer Res.*, 1983, **43**, 3700.
- 6 J. B. Le Pecq, N. Dat-Xuong, C. Gosse and C. Paoletti, *Proc. Natl. Acad. Sci. USA*, 1974, **71**, 5078.
- 7 C. Ducrocq, E. Bisagni, C. Rivalle and J. M. Lhoste, *J. Chem. Soc.*, 1979, **1**, 142.
- 8 Y. A. Lourié, *de mémoire de chimie analytique*, Mir Moscou, 1975.
- 9 S. R. Meech and D. Phillips, *J. Photochem.*, 1983, **23**, 193.
- 10 J. A. Delaire and J. Faure, in *Laser Spectroscopic Methods, Photoinduced Electron Transfer*, Elsevier, New York, 1988, p. 1.
- 11 J. F. Ireland and P. A. H. Wyatt, *Chem. Rev.*, 1976, 134.
- 12 J. Catalan, M. O. Perez and P. Yarez, *J. Mol. Struct.*, 1984, **107**, 263.
- 13 J. Catalan, M. O. Perez and P. Yarez, *Tetrahedron*, 1983, **39**, 2851.
- 14 J. Elguero, C. Marzin, A. R. Katritsky and P. Linda, *The Tautomerism of Heterocycles*, Academic Press, 1976.
- 15 Y. Chen, R. L. Rich, F. Gai and J. W. Petrich, *J. Phys. Chem.*, 1993, **97**, 1770.
- 16 D. Reyman, A. Pardo and J. M. L. Poyato, *J. Phys. Chem.*, 1994, **98**, 10408.
- 17 M. P. Fontaine-Aupart, E. Renault, L. Brian, J. F. Delouis and M. Gardès-Albert, *Photochem. Photobiol.*, 1995, **90**, 95.
- 18 M. A. Schwaller, J. Aubart, F. Sureau, G. Dodin, M. F. Ruasse, R. Leverage, M. F. Poupon and F. Moreau, *L'actualité Chimique*, 1991, 67.
- 19 E. Bardez, A. Chatelain, B. Larrey and B. Valeur, *J. Phys. Chem.*, 1994, **98**, 2357.
- 20 Z. R. Grabowski, K. Rotkiewicz, A. Siemiarz, D. J. Cowley and W. Baumann, *Nouv. J. Chim.*, 1979, **3**, 443.
- 21 W. Rettig, *Angew. Chem.*, 1986, **25**, 971.
- 22 V. K. Kansal and P. Potier, *Tetrahedron*, 1988, **40**, 2389.

Paper 5/06944K

Received 20th October 1995

Accepted 20th March 1996